Thermodynamic analysis of ionizable groups involved in the catalytic mechanism of human matrix metalloproteinase 7 (MMP-7).

AUTHOR(S):

Takeharu, Hitoshi; Yasukawa, Kiyoshi; Inouye, Kuniyo

CITATION:

Takeharu, Hitoshi ...[et al]. Thermodynamic analysis of ionizable groups involved in the catalytic mechanism of human matrix metalloproteinase 7 (MMP-7).. Biochimica et biophysica acta 2011, 1814(12): 1940-1946

ISSUE DATE:

2011-12

URL:

http://hdl.handle.net/2433/151850

BBA - Proteins and Proteomics

Thermodynamic analysis of ionizable groups involved in the catalytic mechanism of human matrix metalloproteinase 7 (MMP-7)

Hitoshi Takeharu, Kiyoshi Yasukawa, Kuniyo Inouye*

Division of Food Science and Biotechnology, Graduate School of Agriculture, Kyoto University, Sakyo-ku, Kyoto 606-8502, Japan

Abbreviations: AMPSO, 3-[(1,1-dimethyl-2-hydroxy-ethyl)amino]-2-hydroxypropane sulfonic acid; DMSO, dimethyl sulfoxide; HEPES, 2-[4-(2-hydroxyethyl)-1-piperazinyl] ethanesulfonic acid; K_e, proton dissociation constant; MES, 2-(*N*-morpholino)ethanesulfonic acid; MMP, matrix metalloproteinase; MOCAc-PLG, (7-methoxycoumarin-4-yl)acetyl-L-Pro-L-Leu-Gly; MOCAc-PLGL(Dpa)AR, (7-methoxycoumarin-4-yl)acetyl-L-Pro-L-Leu-Gly-L-Leu-[N^3-(2,4-dinitrophenyl)-L-2,3-diaminopropionyl]-L-Ala-L-Arg-NH_2.

*Correspondence author. Tel.: +81 75 753 6266; fax: +81 75 753 6265. *E-mail address*: inouye@kais.kyoto-u.ac.jp

Keywords: ionizable group; matrix metalloproteinase; MMP-7; proton dissociation constant; thermodynamic analysis.

Abstract

Human matrix metalloproteinase 7 (MMP-7) exhibits a broad bell-shaped pH-dependence with the acidic and alkaline pK_e (pK_{e1} and pK_{e2}) values of about 4 and 10. In this study, we estimated the ionizable groups involved in its catalytic mechanism by thermodynamic analysis. pK_a of side chains of L-Asp, L-Glu, L-His, L-Cys, L-Tyr, L-Lys, and L-Arg at 25-45°C were determined by the pH titration of amino-acid solutions, from which their enthalpy changes, ΔH^o, of deprotonation were calculated. pK_{e1} and pK_{e2} of MMP-7 at 15-45°C were determined in the hydrolysis of (7-methoxycoumarin-4-yl)acetyl-L-Pro-L-Leu-Gly-L-Leu-[N^3-(2,4-dinitrophenyl)-L-2,3-diaminopropionyl]-L-Ala-L-Arg-NH_2, from which ΔH^o for pK_{e1} and pK_{e2} were calculated. The ΔH^o for pK_{e1} (-20.6 ± 6.1 kJ mol^{-1}) was similar to that for L-Glu (-23.6 ± 5.8 kJ mol^{-1}), and the ΔH^o for pK_{e2} (89.9 ± 4.0 kJ mol^{-1}) was similar to those for L-Arg (87.6 ± 5.5 kJ mol^{-1}) and L-Lys (70.4 ± 4.4 kJ mol^{-1}). The mutation of the active-site residue Glu198 into Ala completely abolished the activity, suggesting that Glu198 is the ionizable group for pK_{e1}. On the other hand, no arginine or lysine residues are found in the active site of MMP-7. We proposed a possibility that a protein-bound water is the ionizable group for pK_{e2}.

1. Introduction

Human matrix metalloproteinase 7 (MMP-7, Matrilysin) [EC 3.4.24.23] is the smallest matrix metalloproteinase (MMP), lacking a carboxyl terminal hemopexin-like domain conserved in common MMPs. It is believed to play an important role in tumor invasion and metastasis [1, 2]. The molecular mass of the latent pro-form is 28 kDa, and that of its mature form is 19 kDa [3]. MMP-7 is composed of a five-stranded β-sheet and three α-helices, and contains a zinc ion essential for activity and other zinc and calcium ions that are considered necessary for stability [4]. Like all other MMPs, it has the consensus sequence HEXXHXXGXXH, in which three histidine residues chelate a catalytic zinc ion, and a methionine-containing turn (Met-turn). Hence, it is grouped in clan MA(M) [5]. In recent years, target molecules through which MMP-7 exerts biological functions have become apparent, such as heparin [6], heparan sulfate [6], cholesterol sulfate [7-9], and ErbB4 receptor [10]. The inhibitions of MMP-7 activity by natural compounds [11,12], synthetic compounds [13], and detergents [14] were reported.

Generally, ionizable groups involved in the catalytic mechanisms of enzyme are estimated from the three-dimensional structure and pK_e values. Figure 1A shows the structure of MMP-7-hydroxamate inhibitor complex [4]. In this study, the numbering of amino acid residues of pro-MMP-7 is according to the previous report [15], in which the mature MMP-7 begins at Tyr78. MMP-7 has three α helices and five β strands [4]. Tyr193 and Glu198 are located at the second α-helix (Leu192-Leu203), while Tyr216 and Tyr219 are located at the Met-turn (Pro211-Gly222). Sequence comparison of MMP-1 [16], MMP-2 [17], MMP-3 [18], MMP-7 [19], MMP-8 [20], MMP-9 [21],

MMP-10 [19], MMP-11 [22], MMP-12 [21], MMP-13 [21], and MMP-14 [23] revealed that Glu198 and Tyr219 are conserved in all MMPs, while Tyr216 is conserved in several MMPs, and Tyr193 is unique to MMP-7 [24]. Tyr219 and Tyr216 form the S1' subsite. MMP-7 exhibits a broad bell-shaped pH-dependence with the acidic and alkaline pK_e (pK_{e1} and pK_{e2}) values of about 4 and 10 [13,25]. As a result, three ionization forms of MMP-7 and MMP-7-substrate complex are considered, respectively (Fig. 2). Glu198 and Tyr219 are believed to be the ionizable groups responsible for pK_{e1} and pK_{e2}, respectively. However, Cha *et al.* proposed that the zinc-bound water might be the ionizable group responsible for pK_{e1} [26]. We found that the MMP-7 whose tyrosyl residues were nitrated with tetranitromethane retained activity [27]. In addition, we recently demonstrated that all Tyr219 variants retained activity [28]. These results indicate that Tyr219 is not critical for catalytic activity. We also demonstrated that Tyr193 and Tyr216 variants retained activity [28].

One of the critical problems with using pK_a values of free amino acids for estimation of charge states of amino acid residues is that little water (and hence protons) is available for the residues buried in a protein core, while large amounts of water (55 M water) is available for the residues facing bulk solution. In 1930-1960, enthalpy changes, ΔH^o, of deprotonation of side chains of amino acid residues were determined by the measurement of pH- and temperature-dependences of electromotive force of the battery containing amino acids, dipeptides, or tripeptides in a cell [29-33]. It was demonstrated that in dipeptides and tripeptides, ΔH^o values of side chains of amino acid residues are not affected by the amino acid residues in their neighborhoods and are almost equal to the ΔH^o values of side chains of free amino acids [29-33]. Therefore, ΔH^o values can be used as a clue to estimate the ionizable groups in the catalytic mechanism of enzymes

[29,34-36]. However, compared with the estimation of the ionizable groups with pK_e values, the estimation with ΔH^o values is not commonly used. This might be due to that reliable ΔH^o values of side chains of amino acid residues have not been available. In this study, we determined the ΔH^o of side chains of amino acid residues by the pH-titration of amino-acid solutions and used them to estimate the ionizable groups involved in the catalytic mechanism of MMP-7.

2. Materials and methods

2.1. Materials

(7-methoxycoumarin-4-yl)acetyl-L-Pro-L-Leu-Gly-L-Leu-[N^3-(2,4-dinitrophenyl)-L-2,3-diaminopropionyl]-L-Ala-L-Arg-NH_2 [MOCAc-PLGL(Dpa)AR] (Lot 491214, molecular mass 1093.2 Da) [37] and (7- methoxycoumarin-4-yl)acetyl-L-Pro-L-Leu-Gly (MOCAc-PLG) (Lot 510913, molecular mass 501.54 Da) were purchased from the Peptide Institute (Osaka, Japan). Their concentrations were determined by the denoted weight and the molecule weight. 3-[(1,1-Dimethyl-2-hydroxy-ethyl)amino]-2-hydroxypropane sulfonic acid (AMPSO, Lot 9355C, molecular mass 227.3 Da) and L-Glu (Lot TLE5153) were from Wako Pure Chemical (Osaka). L-Asp (Lot 115H0563) and N^α-acetyl-L-Lys (Lot A1020) were from Sigma (St. Louis, MO, USA). L-His (Lot M2N7937), L-Cys (Lot M7H2081), L-Tyr, (Lot M7K3391), and L-Arg (Lot M7K6540) were from Nacalai Tesque (Kyoto, Japan). All other chemicals were from Nacalai Tesque.

118 *2.2. Expression and purification of MMP-7*

119

120 Expression in *Escherichia coli* and purification of recombinant MMP-7 were
121 carried out, as described previously [31,39]. Briefly, mature MMP-7 (Met77-Lys250)
122 was expressed in BL21(DE3) cells in the forms of inclusion bodies, solubilized with 6
123 M guanidine HCl, refolded with 1 M L-arginine, and purified by sequential ammonium
124 sulfate precipitation and heparin affinity column-chromatography procedures of the
125 refolded products. The concentration of MMP-7 was determined spectrophotometrically
126 using the molar absorption coefficient at 280 nm, ε_{280}, of 31,800 M^{-1} cm^{-1} [38].
127 Site-directed mutagenesis was carried out using Quikchange™ site-directed
128 mutagenesis kit (Stratagene, La Jolla, CA) for construction of E198A, A162G, and
129 P217G. The nucleotide sequences of mutated MMP-7 genes were verified by a
130 Shimadzu DNA sequencer DSQ-2000 (Kyoto).

131

132 *2.3. Fluorometric analysis of hydrolysis of MOCAc-PLGL(Dpa)AR*

133

134 The MMP-7-catalyzed hydrolysis of MOCAc-PLGL(Dpa)AR was initiated by
135 mixing 1222 μl of the reaction buffer, 20 μl of the MMP-7 solution (625 nM), and 8 μl
136 of the substrate solution (234 μM) dissolved in DMSO. The initial concentrations of
137 enzyme, MOCAc-PLGL(Dpa)AR, and DMSO were 10 nM, 1.5 μM, and 0.64% (v/v),
138 respectively. The reaction buffers were 50 mM acetate-NaOH buffer at pH 3.6-5.8, 50
139 mM MES-NaOH buffer at pH 5.6-7.0, 50 mM HEPES-NaOH buffer at pH 6.8-8.6, and
140 50 mM AMPSO-NaOH buffer at pH 8.6-10.4, each containing 10 mM $CaCl_2$. The
141 reaction was measured by following the increase in the fluorescence intensity at 393 nm

with excitation at 328 nm with a JASCO FP-777 fluorescence spectrophotometer (Tokyo, Japan). The peptide bond of Gly-L-Leu residues was cleaved by MMP-7, and the amount of the product MOCAc-PLG was estimated by the fluorescence intensity by comparison with the fluorescence intensity of an authentic MOCAc-PLG solution. The hydrolysis was carried out under pseudo-first order conditions, where the initial concentration of MOCAc-PLGL(Dpa)AR (1.5 μM) was much lower than K_m (60 μM) [38]. The Michaelis-Menten equation is, then, expressed as Eq. 1.

$$v_o = (k_{cat}/K_m)[E]_o[S]_o \quad (1)$$

where v_o, k_{cat}, $[E]_o$, and $[S]_o$ mean the initial reaction rate, the molecular activity, the initial enzyme concentration, and the initial substrate concentration, respectively. The kinetic parameters, the intrinsic k_{cat}/K_m, $(k_{cat}/K_m)_o$, and the proton dissociation constants (K_{e1} and K_{e2}) for pH-dependence of the activity were calculated from Eq. 2 by a non-linear least squares regression method with Kaleida Graph Version 3.5 (Synergy Software, Essex, VT).

$$(k_{cat}/K_m)_{obs} = \frac{(k_{cat}/K_m)_o}{1 + \frac{[H^+]}{K_{e1}} + \frac{K_{e2}}{[H^+]}} \quad (2)$$

In this equation, $(k_{cat}/K_m)_{obs}$ and [H] mean the k_{cat}/K_m value observed and the proton concentration, respectively, at the specified pH.

2.4. Thermodynamic analysis of K_{e1} and K_{e2}

The enthalpy changes, ΔH^o, of deprotonation were calculated from pK_e shifts using Eq. 3, known as the van't Hoff equation,

$$\frac{d\,(\ln K_e)}{dT} = \frac{\Delta H^o}{RT^2} \qquad (3)$$

where T and R mean the absolute temperature in degrees Kelvin and the gas constant (= 8.314 J K^{-1} mol^{-1}), respectively. When this equation is integrated, it is expressed as Eq. 4,

$$-\log K_e = \frac{\Delta H^o}{2.303\,RT} + A \qquad (4)$$

where A means the constant of integration. Thus, a slope of a plot for pK_e values versus $1/T$ gives ΔH^o.

2.5. Titration of pH of amino-acid solution and thermodynamic analysis of proton dissociation constant of side chains of amino acids

Amino acid was dissolved in water to be 10 mM for L-Asp, L-Glu, L-His, L-Cys, and L-Arg and 1 mM for L-Tyr and N^{α}-acetyl-L-Lys. Titration was made with 50 or 100 µl of 2 M HCl or 2 M NaOH for each amino-acid solution (500 ml) incubated at 25, 35, or 45ºC as follows: the L-Asp and L-Glu solutions were titrated with NaOH until pH reached 6.0. The L-His solution was titrated with HCl until pH reached 3.0. The L-Cys solution was titrated with HCl until pH reached 6.8. The L-Arg solution was titrated

with HCl until pH reached 9.8. The L-Tyr solution was titrated with HCl until pH reached 7.5. The N^{α}-acetyl-L-Lys solution was titrated with HCl until pH reached 9.2.

The following is the case with L-Glu, as an example. Based on the previous reports that pK_a values of α-COOH and γ-COOH of L-Glu at 25ºC are around 2.0 and 4.0, respectively [29-33], the course of a titration of L-Glu with NaOH from pH 2 to 6 can be represented in the following schemes.

$$H_3N^+(CH(CH_2)_2COOH)COOH + OH^- \rightarrow H_3N^+(CH(CH_2)_2COOH)COO^- + H_2O$$

$$H_3N^+(CH(CH_2)_2COOH)COO^- + OH^- \rightarrow H_3N^+(CH(CH_2)_2COO^-)COO^- + H_2O$$

The degree of dissociation, α, is defined as the following equation,

$$\alpha = \frac{2[H_3N^+(CH(CH_2)_2COO^-)COO^-] + [H_3N^+(CH(CH_2)_2COOH)COO^-]}{C} \quad (5)$$

where C means the initial concentration of L-Glu. The α □value increases up to 2 in the course of the titration. The electric balance is given by the following equation.

$$[H^+] + [Na^+] + [H_3N^+(CH(CH_2)_2COOH)COOH] =$$

$$[OH^-] + [Cl^-] + [H_3N^+(CH(CH_2)_2COO^-)COO^-] \quad (6)$$

Substituting Eq. 5 into Eq. 6 yields the following equation,

$$\alpha = \frac{C-[H^+]+[Na^+]-K_w/[H^+]-[Cl^-]}{C} \quad (7)$$

where K_w is ionic product. The α□ at each pH was calculated from Eq. 7. K_{a1} and K_{a2}, which are defined as Eqs. 8 and 9, respectively, were calculated from Eq. 10 by a non-linear least squares regression method with Kaleida Graph Version 3.5.

$$K_{a1} = \frac{[H^+]\,[H_3N^+(CH(CH_2)_2COOH)COO^-]}{[H_3N^+(CH(CH_2)_2COOH)COOH]} \quad (8)$$

$$K_{a2} = \frac{[H^+]\,[H_3N^+(CH(CH_2)_2COO^-)COO^-]}{[H_3N^+(CH(CH_2)_2COOH)COO^-]} \quad (9)$$

$$\alpha = \frac{2 + \dfrac{[H^+]}{K_{a2}}}{1 + \dfrac{[H^+]}{K_{a2}} + \dfrac{[H^+]^2}{K_{a1}\,K_{a2}}} \quad (10)$$

ΔH^o of deprotonation of side chains of L-Glu was calculated from pK_{a2} shift using Eq. 3.

3. Results

3.1. ΔH^o values of deprotonation of side chains of amino acids

The wild-type MMP-7 was prepared as described in Materials and methods section. Starting with 100 ml of *E. coli* cultures, 2 mg purified enzyme was recovered. Upon SDS-PAGE under reducing conditions, each yielded a single band with a molecular

225 mass of 19 kDa (data not shown).

226 To determine ΔH^o values of deprotonation of side chains of amino acids, we made
227 a titration of pH of L-Asp, L-Glu, L-His, L-Cys, L-Tyr, N^{α}-acetyl-L-Lys, and L-Arg
228 solutions. The result with L-Glu is shown in Fig. 3, as an example. The degree of
229 dissociation, α, which is defined as Eq. 5, increased rapidly with an increase of pH from
230 1.9 to 2.5, gradually with the increase from 2.5 to 3.8, and rapidly again with the
231 increase from 3.8 to 4.5. The pK_{a1} and pK_{a2} were calculated by Eq. 10 to be 2.1 ± 0.1
232 and 4.0 ± 0.1 for 25°C, 2.2 ± 0.1 and 4.1 ± 0.1 for 35°C, and 2.3 ± 0.1 and 4.2 ± 0.1 for
233 45°C, respectively. The pK_{a1} was assigned to α-carboxyl group, and the pK_{a2} was
234 assigned to the side chain of L-Glu, based on the previous reports [29-33]. ΔH^o for the
235 pK_{a2} was calculated by the van't Hoff plot to be -23.6 ± 5.8 kJ mol^{-1} (inset of Fig. 3). All
236 results are summarized in Table 1. The ΔH^o of the side chains of L-Asp and L-Glu were
237 negative, while those of the other five positive. The ΔH^o of the side chains of L-Asp,
238 L-His, and L-Cys were almost the same as the ones previously reported, which were
239 determined by measuring the pH- and temperature-dependences of electromotive force
240 of the battery containing amino acids or dipeptides in the cell (-6 to 6 kJ mol^{-1} for L-Asp
241 [29], 29-32 kJ mol^{-1} for L-His [31], and 24-26 kJ mol^{-1} for L-Cys [33]). On the other
242 hand, the ΔH^o of the side chains of the other four were substantially different from the
243 ones previously reported (-6 to 6 kJ mol^{-1} for L-Glu [29], 25-26 kJ mol^{-1} for L-Tyr [31],
244 44-55 kJ mol^{-1} for L-Lys [31], and 50-52 kJ mol^{-1} for L-Arg [31]).

245

246 *3.2. ΔH^o of deprotonation of ionizable groups responsible for pK_{e1} and pK_{e2} of MMP-7*

247

248 According to Fig. 2 and Eq. 2, the pH dependence of k_{cat}/K_m results from the

association and dissociation of proton in the free MMP-7, but not the MMP-7 combined with substrate. The k_{cat}/K_m values of MMP-7 in the hydrolysis of MOCAc-PLGL(Dpa)AR in the pH range of 3.6-10.4 at 15, 25, 35, and 45°C were determined by Eq. 1 and are shown in Fig. 4. All plots showed bell-shaped curves. The plot at 15°C showed the widest active pH-range while that at 45°C showed the narrowest. The intrinsic k_{cat}/K_m, $(k_{cat}/K_m)_o$, and the pK_e values were determined by Eq. 2, which are summarized in Table 2. The $(k_{cat}/K_m)_o$ value was the lowest at 15°C and the highest at 45°C. Figure 5 shows van't Hoff plot for pK_{e1} and pK_{e2}. ΔH^o of deprotonation were calculated to be -20.6 ± 6.1 kJ mol^{-1} for pK_{e1} and 89.9 ± 4.0 kJ mol^{-1} for pK_{e2}.

3.3. Estimation of the ionizable groups responsible for pK_{e1} and pK_{e2} of MMP-7

By comparison with the ΔH^o of MMP-7 (-20.6 ± 6.1 kJ mol^{-1} for pK_{e1} and 89.9 ± 4.0 kJ mol^{-1} for pK_{e2}) with the ΔH^o of side chains of amino acids (Table 1), glutamate residue was thought to be the ionizable group responsible for pK_{e1}, and arginine or lysine residue for pK_{e2}. This suggested that Glu198 is the ionizable group for pK_{e1} (Fig. 1), as previously pointed out [4]. However, no arginine or lysine residues are found in the active site (Fig. 1). We therefore hypothesized that a protein-bound water is the ionizable group for pK_{e2}.

3.4. Water molecules as the candidate for ionizable group responsible for pK_{e2}

The hydroxamate (R-CO-NH-OH) peptide mimetic inhibitor, which binds covalently to the active-site zinc ion, is the first MMP inhibitor [40]. In the

MMP-7-hydroxamate inhibitor complex (Protein Data Bank no. 1MMQ) [4], we noticed two water molecules (W1 and W2) as the possible candidates for the ionizable group responsible for pK_{e2} (Fig. 1B), based on the following reasons: (i) W1 and W2 are located 2.7 Å far from each one of the two oxygen atoms of hydroxamate bound to the active site zinc ion; (ii) W1 binds to the main-chain nitrogen atom of Ala162, and W2 binds to the main-chain carbonyl oxygen atom of Pro217. Ala162 is located at the fourth β-sheet (Ala162-Ala164) of MMP-7, and Pro217 is located at the Met-turn (Pro211-Gly222). Both Ala162 and Pro217 are conserved among MMPs; and (iii) In the X-ray crystallographic structure of MMP-7 complexed with carboxylate inhibitor (1MMP) and sulfodiimine inhibitor (1MMR), the water molecules corresponding to W1 and W2 are found [4].

3.5. Kinetic analysis of the MMP-7 variants

To see if the ionizable group responsible for pK_{e1} is Glu198, we constructed the MMP-7 variant, E198A. To explore the possibility that either W1 or W2 is the ionizable group responsible for pK_{e2}, we constructed the variants, A162G and P217G, assuming that the main-chain structure of MMP-7 could be changed by mutating Ala162 or Pro217 into glycine, which is the most flexible amino acid residue, and that such mutation alters pK_{e2} if the ionizable group responsible for pK_{e2} is located in the neighborhood of the site of mutation. The variants were produced in the *E. coli* expression system [38]. The pH-dependence of the k_{cat}/K_m of the wild-type MMP-7, E198A, A162G, and P217G in the hydrolysis of MOCAc-PLGL(Dpa)AR at 25°C is shown in Fig. 6, and the kinetic parameters are summarized in Table 3. E198A

completely lacked the activity. To see if it retained small MOCAc-PLGL(Dpa)AR-hydrolyzing activity, we made HPLC analysis [27]. No activity was detected in E198A even with the enzyme and substrate concentrations of 1 μM and 140 μM, respectively, and the reaction time of 120 min (data not shown). On the other hand, the activity was detected in the wild-type enzyme with the enzyme and substrate concentrations of 1 nM and 140 μM, respectively, and the reaction time of 10 min (data not shown). This indicated that the activity of E198A, if any, was less than 0.01% of that of the wild-type enzyme, suggesting that E198A completely lost the activity and that Glu198 is not the ionizable group responsible for pK_{e1}.

A162G and P217G retained the activity with the $(k_{cat}/K_m)_o$ values of 57% and 78% of that of the wild-type enzyme, respectively (Table 3). The pK_{e1} of A162G and P217G were 4.9 ± 0.1 and 5.3 ± 0.1, being higher by 0.3 ± 0.2 and 0.7 ± 0.2 unit, respectively, than that of the wild-type enzyme (4.6 ± 0.1). The pK_{e2} of A162G and P217G were 10.3 ± 0.1 and 10.0 ± 0.1, being higher by 0.6 ± 0.2 and 0.3 ± 0.2 unit, respectively, than that of the wild-type enzyme (9.7 ± 0.1). These results indicated that the mutations of Ala162→Gly and Pro217→Gly affected the electrostatic environment of the ionizable groups responsible for not only pK_{e2} but also pK_{e1}.

4. Discussion

4.1. Estimation of ionizable groups involved in the catalytic mechanism of MMP-7

Browner et al. proposed that, based on the crystal structure of the complex of MMP-7 and its inhibitor, Glu198 is the ionizable group responsible for pK_{e1}: it functions

both as a base and an acid, deprotonating the zinc-bound water and transferring the proton to the leaving amine [4]. Cha et al. proposed that, based on the pH-dependence of the activity, Tyr219 is the ionizable group responsible for pK_{e2}: the ionized side chain of Tyr219 makes the active site of MMP-7 hydrophilic [25]. They also proposed that the zinc-bound water, but not Glu198, is the ionizable group responsible for pK_{e1}: the ionized zinc-bound water molecule attacks the carbonyl carbon of the scissile bond as a nucleophile [26]. We demonstrated that, based on the results with chemical modification [27] and site-directed mutagenesis [28], Tyr219 is not the ionizable group responsible for pK_{e2}.

Thermodynamic analysis in this study suggested that glutamate residue is the ionizable group for pK_{e1}, and that arginine or lysine residue is that for pK_{e2} (Tables 1 and 2). The mutation of Glu198→Ala completely abolished activity (Table 3). We think that E198A has similar three-dimensional folds to the wild-type MMP-7 because the expression level and stability of E198A were similar to those of the wild-type MMP-7: starting from 100-ml culture, 2 mg purified E198A was obtained by the denaturation and refolding processes. Purified E198A was stable on storage at 4°C. On the other hand, some MMP-7 variants precipitated during the refolding process (K. Y. and K. I., unpublished data). Although it is difficult to exclude a possibility that the loss of activity by the mutation Glu198→Ala does not result from the structural change, our result suggests that Glu198 is the ionizable group responsible for pK_{e1}. This agrees well with the previous reports that in MMP-1 [41], MMP-3 [42], and MMP-9 [43], the glutamate residue corresponding to Glu198 of MMP-7 is catalytically important. On the other hand, arginine and lysine residue were declined for the ionizable group for pK_{e2} because there are no lysine or arginine residues in the active site. We therefore proposed that a

345 protein-bound water is the ionizable group for pK_{e2}. We noticed two water molecules,
346 Ala162-bound water (W1) and Pro217-bound water (W2), as the candidates for the
347 ionizable group for pK_{e2}. The mutations of Ala162→Gly and Pro217→Gly altered not
348 only pK_{e2} but also pK_{e1} values. This indicated that the mutations affected the
349 electrostatic environment of the active site. To further explore our hypothesis, extensive
350 site-directed mutagenesis study is required.
351
352 *4.2. Catalytic mechanism of MMP-7*
353
354 Based on the results in this study, we propose the following catalytic mechanism of
355 MMP-7 (Fig. 7). In free enzyme, Glu198 must be in its deprotonated state and the
356 protein-bound water must be in its unionized state for catalysis (Fig. 7A). The Michaelis
357 complex is formed when the carbonyl oxygen of the scissile bond binds the zinc ion.
358 Zinc ion polarizes the carbonyl group of the scissile bond. Glu198 accepts a proton from
359 the zinc-bound water (Fig. 7B). The tetrahedral complex is formed when the ionized
360 zinc-bound water attacks the carbonyl carbon of the scissile bond, and then stabilized by
361 the interaction between the carbonyl oxygen of the scissile bond and the oxygen of the
362 protein-bound water in its unionized state (Fig. 7C). This stabilization does not occur
363 when this protein-bound water is negatively charged. The amino product is released
364 when Glu198 transfers the proton to the nitrogen of the scissile bond (Fig. 7D).
365 pK_a of free water is 15.7. The above mechanism is consistent with the pH
366 dependence of MMP-7 activity with pK_{e1} and pK_{e2} values of 4.0 and 9.8 if the pK_a of
367 the protein-bound water greatly decreases. The zinc-bound water should be released in
368 the MMP-7-hydroxamate inhibitor complex (Protein Data Bank no. 1MMQ) [4]

because hydroxamate (R-CO-NH-OH) binds to the zinc ion as the bidentate ligand. When the substrate coordinates to the zinc ion through the mono dentate ligand such as the carbonyl oxygen of the scissile bond, it still binds to the zinc ion. Therefore, it is thought that the pK_a of the zinc-bound water also greatly decreases. Considering the mechanism that the ionized zinc-bound water attacks the carbonyl carbon of the scissile bond (Fig. 7), it is thought that the ionizable group responsible for pK_{e2} is the protein-bound, but not zinc-bound, water.

It should be mentioned that in MMP-3, the protein-bound water involved in the catalytic mechanism was in its protonated state for catalysis, stabilizing the tetrahedral intermediate by coordinating the carbonyl oxygen of the scissile bond of the substrate [44]. In carboxypeptidase A, which belongs to Clan MC of zinc metalloproteinase, the ionizable group for pK_{e1} of 7 was assigned to the active-site glutamate residue, and that for pK_{e2} of 10 was assigned to the zinc-bound water molecule [45]. It was thought that the active-site glutamate residue functions as a general base while the zinc-bound water is in its unionized state, stabilizing the tetrahedral intermediate [45].

4.3. Estimation of the ionizable groups involved in the catalytic mechanism of enzymes by ΔH^o of deprotonation

pK_a of active-site residues can vary depending on their microenvironment. To our knowledge, the highest pK_a of the active-site glutamate residue is 8.4 in xylanase [46], suggesting that it is difficult to estimate the ionizable groups of enzymes only by their pK_a values. In this study, we determined pK_a of side chains of L-Asp, L-Glu, L-His, L-Cys, L-Tyr, L-Lys, and L-Arg at 25-45°C by the pH titration of amino-acid solutions,

from which we calculated ΔH^o of deprotonation. In the previous reports [29], ΔH^o of side chains of L-Asp and L-Glu were the same (in the range of -6 to 6 kJ mol^{-1}). In this study, they were different (-6.4 ± 3.5 kJ mol^{-1} for L-Asp and -23.6 ± 5.8 kJ mol^{-1} for L-Glu) (Table 1). Considering that the ionizable group for pK_{e1} can be assigned to Glu198 by the ΔH^o value (-20.6 ± 6.1 kJ mol^{-1}), the ΔH^o of side chains of amino acids presented in this study might be a powerful tool to estimate the ionizable groups involved in the catalytic mechanism of various enzymes.

In conclusion, we propose that Glu198 and unidentified protein-bound water are the ionizable groups involved in the catalytic mechanism of MMP-7. To identify the protein-bound water, site-directed mutagenesis study of MMP-7 is currently underway.

Acknowledgements

This study was supported in part (K. I.) by Grants-in-Aid for Scientific Research (Nos. 17380065 and 20380061) from the Japan Society of the Promotion of Science.

References

[1] J.F. Woessner, Jr., Matrix metalloproteinases and their inhibitors in connective tissue remodeling. FASEB J. 5 (1991) 2145-2154.

[2] H. Nagase, J.F. Woessner, Jr., Matrix metalloproteinases. J. Biol. Chem. 274 (1999) 21491-21494.

[3] J.F. Woessner, Jr., C.J. Taplin, Purification and properties of a small latent matrix metalloproteinase of the rat uterus. J. Biol. Chem. 263 (1988) 16918-16925.

[4] M.F. Browner, W.W. Smith, A.L. Castelhano, Matrilysin-inhibitor complexes: common themes among metalloproteinases. Biochemistry 34 (1995) 6602-6610.

[5] N.D. Rawlings, F.R., Morton, C.Y. Kok, J. Kong, A.J. Barrett, MEROPS: the peptidase database. Nucleic Acids Res. 36 (2008) D320-D325.

[6] W.-H. Yu, J.F. Woessner, Jr., Heparan sulfate proteoglycans as extracellular docking molecules for matrilysin (matrix metalloproteinase 7). J. Biol. Chem. 275 (2000) 4183-4191.

[7] K. Yamamoto, S. Higashi, M. Kioi, J. Tsunezumi, K. Honke, K. Miyazaki, Binding of active matrilysin to cell surface cholesterol sulfate is essential for its membrane-associated proteolytic action and induction of homotypic cell adhesion. J. Biol. Chem. 281 (2006) 9170-9180.

[8] S. Higashi, M. Oeda, K. Yamamoto, K. Miyazaki, Identification of amino acid residues of matrix metalloproteinase 7 essential for binding to cholesterol sulfate. J. Biol. Chem. 283 (2008) 35735-35744.

[9] K. Yamamoto, K. Miyazaki, S. Higashi, Cholesterol sulfate alters substrate preference of matrix metalloproteinase-7 and promotes degradations of pericellular laminin-332 and fibronectin. J. Biol. Chem. 285 (2010) 28862-28873.

[10] C.C. Lynch, T. Vargo-Gogola, M.D. Martin, B. Fingleton, H.C. Crawford, L.M. Matrisian, Matrix metalloproteinase 7 mediates mammary epithelial cell tumorigenesis through the ErbB4 receptor. Cancer Res. 57 (2007) 6760-6767.

[11] H. Oneda, M. Shiihara, K. Inouye, Inhibitory effects of green tea catechins on the activity of human matrix metalloproteinase 7 (matrilysin). J. Biochem. 133 (2003) 571-576.

[12] Y. Muta, S. Oyama, T. Umezawa, M. Shimada, K. Inouye, Inhibitory effects of

441 lignans on the activity of human matrix metalloproteinase 7 (matrilysin). J. Agric. Food
442 Chem. 52 (2004) 5888-5894.
443 [13] H. Oneda, K. Inouye, Interactions of human matrix metalloproteinase 7
444 (matrilysin) with the inhibitors thiorphan and R-94138. J. Biochem. 129 (2001)
445 429-435.
446 [14] H.I. Park, S. Lee, A. Ullah, Q. Cao, Q.X. Sang, Effects of detergents on catalytic
447 activity of human endometase/matrilysin 2, a putative cancer biomarker. Anal. Biochem.
448 396 (2010) 262-268.
449 [15] T. Crabbe, F. Willenbrock, D. Eaton, P. Hynds, A.F. Carne, G. Murphy, A.J.
450 Docherty, Biochemical characterization of matrilysin. Activation conforms to the
451 stepwise mechanisms proposed for other matrix metalloproteinases. Biochemistry 31
452 (1992) 8500-8507.
453 [16] G.I. Goldberg, S.M. Wilhelm, A. Kronberger, E.A. Bauer, G.A. Grant, A.Z. Eisen,
454 Human fibroblast collagenase. Complete primary structure and homology to an
455 oncogene transformation-induced rat protein. J. Biol. Chem. 261 (1986) 6600-6605.
456 [17] B. Birkedal-Hansen, W.G. Moore, R.E. Taylor, A.S. Bhown, H. Birkedal-Hansen,
457 Monoclonal antibodies to human fibroblast procollagenase. Inhibition of enzymatic
458 activity, affinity purification of the enzyme, and evidence of clustering epitopes in the
459 NH_2-terminal end of the activated enzyme. Biochemistry 27 (1988) 6751-6758.
460 [18] S.E. Whitham, G. Murphy, P. Angel, H.J. Rahmsdorf, B.J. Smith, A. Lyons, T.J.
461 Harris, J.J. Reynolds, P. Herrlich, A.J. Docherty, Comparison of human stromelysin and
462 collagenase by cloning and sequence analysis. Biochem. J. 240 (1986) 913-916.
463 [19] D. Muller, B. Quantin, M.C. Gesnel, R. Millon-Collard, J. Abecassis, R.
464 Breathnach, The collagenase gene family in humans consists of at least four members.

Biochem. J. 253 (1988) 187-192.

[20] P. Devarajan, K. Mookhtiar, H. van Wart, N. Berliner, Structure and expression of the cDNA encoding human neutrophil collagenase. Blood 77 (1991) 2731-2738.

[21] H. Birkedal-Hansen, W.G. Moore, M.K. Bodden, L.J. Windsor, B. Birkedal-Hansen, A. DeCarlo, J.A. Engler, Matrix metalloproteinases: a review. Crit. Rev. Oral Biol. Med. 4 (1993) 197-250.

[22] P. Basset, J.P. Bellocq, C. Wolf, I. Stoll, P. Hutin, J.M. Limacher, O.L. Podhajcer, M.P. Chenard, M.C. Rio, P. Chambon, A novel metalloproteinase gene specifically expressed in stromal cells of breast carcinomas. Nature 348 (1990) 699-704.

[23] T. Takino, H. Sato, E. Yamamoto, M. Seiki, Cloning of a human gene potentially encoding a novel matrix metalloproteinase having a C-terminal transmembrane domain. Gene 155 (1995) 293-298.

[24] Q.A. Sang, D.A. Douglas, Computational sequence analysis of matrix metalloproteinase. J. Protein Chem. 15 (1996) 137-160.

[25] J. Cha, M.V. Pedersen, D.S. Auld, Metal and pH dependence of heptapeptide catalysis by human matrilysin. Biochemistry 35 (1996) 15831-15838.

[26] J. Cha, D.S. Auld, Site-directed mutagenesis of the active site glutamate in human matrilysin: investigation of its role in catalysis. Biochemistry 36 (1997) 16019-16024.

[27] Y. Muta, H. Oneda, K. Inouye, Anomalous pH-dependence of the activity of human matrilysin (matrix metalloproteinase-7) as revealed by nitration and amination of its tyrosine residues. Biochem. J. 386 (2005) 263-270.

[28] Y. Muta, K. Inouye, Tyr219 of human matrix metalloproteinase 7 (MMP-7) is not critical for catalytic activity, but is involved in the broad pH-dependence of the activity. J. Biochem. in press

[29] J.T. Edsall, Dipolar ions and acid-base equilibria in: E.J. Cohn, J.T. Edsall (Eds.), Proteins, amino acids, and peptides as ions and dipolar ions, Hafner Publishing Company, New York and London, 1943, pp. 75-115.

[30] J.P. Geenstein, Studies of the peptides of trivalent amino acids. I. Titration constants of histidyl-histidine and of aspartyl-aspartic acid. J. Biol. Chem. 93 (1931) 479-494.

[31] J.P. Greenstein, Studies of the peptides of trivalent amino acids. III. The apparent dissociation constants, free energy changes, and heats of ionization of peptides involving arginine, histidine, lysine, tyrosine, and aspartic and glutamic acids, and the behavior of lysine peptides toward nitrous acid. J. Biol. Chem. 101 (1933) 603-621.

[32] P.K. Smith, A.C. Taylor, E.R.B. Smith, Thermodynamic properties of solutions of amino acids and related substances. III. The ionization of aliphatic amino acids in aqueous solution from one to fifty degrees. J. Biol. Chem. 122 (1937) 109-123.

[33] R. Cecil, J.R. McPhee, A kinetic study of the reactions on some disulphides with sodium sulphite. Biochem. J. 60 (1955) 496-506.

[34] K. Hiromi, K. Takahashi, Z. Hamauzu, S. Ono, Kinetic studies on gluc-amylase. III. The influence of pH on the rates of hydrolysis of maltose and panose. J. Biochem. 59 (1966) 469-475.

[35] W.J. Zhu, M. Li, X.Y. Wang, Chemical modification studies on arginine kinase: essential cysteine and arginine residues at the active site. Int. J. Biol. Macromol. 41 (2007) 564-571.

[36] M.Y. Kondo, D.N. Okamoto, J.A. Santos, M.A. Juliano, K. Oda, B. Pillai, M.N. James, L. Juliano, I.E. Gouvea, Studies on the catalytic mechanism of glutamic peptidase. J. Biol. Chem. 285 (2010) 21437-21445.

513 [37] C.G. Knight, F. Willenbrock, G. Murphy, A novel coumarin-labelled peptide for
514 sensitive continuous assays of the matrix metalloproteinase. FEBS Lett. 296 (1992)
515 263-266.
516 [38] Y. Muta, N. Yasui, Y. Matsumiya, M. Kubo, K. Inouye, Expression in *Escherichia*
517 *coli*, refolding, and purification of the recombinant mature form of human matrix
518 metalloproteinase 7 (MMP-7). Biosci. Biotechnol. Biochem. 74 (2010) 2151-2517.
519 [39] H. Oneda, K. Inouye, Refolding and recovery of recombinant human matrix
520 metalloproteinase 7 (matrilysin) from inclusion bodies expressed by *Escherichia coli*. J.
521 Biochem. 126 (1999) 905-911.
522 [40] M. Betz, P. Huxley, S.J. Davies, Y. Mushtaq, M. Pieper, H. Tschesche, W. Bode,
523 F.X. Comis-Rüth, 1.8-Å crystal structure of the catalytic domain of human neutrophil
524 collagenase (matrix metalloproteinase-8) complexed with a peptidomimetic
525 hydroxamate primed-side inhibitor with a distinct selectivity profile. Eur. J. Biochem.
526 247 (1997) 356-363.
527 [41] L.J. Windsor, M.K. Bodden, B. Birkedal-Hansen, J.A. Engler, H. Birkedal-Hansen,
528 Mutational analysis of residues in and around the active site of human fibroblast-type
529 collagenase. J. Biol. Chem. 269 (1994) 4033-4040.
530 [42] B. Arza, M. de Maeyer, J. Félez, D. Collen, H.R. Lijnen, H.R. (2001) Critical role
531 of glutamic acid 202 in the enzyme activity of stromelysin-1 (MMP-3). Eur. J. Biochem.
532 268 (2001) 826-831
533 [43] S. Rowsell, P. Hawtin, C.A. Minshull, H. Jepson, S.M. Brockbank, D.G. Barratt,
534 A.M. Slater, W.L. McPheat, D. Waterson, A.M. Henney, R.A. Pauptit, Crystal structure
535 of human MMP9 in complex with a reverse hydroxamate inhibitor. J. Mol. Biol. 319
536 (2002) 173-181.

[44] V. Pelmenschikov, P.E. Siegbahn, Catalytic mechanism of matrix metalloproteinases: two-layered ONIOM study. Inorg. Chem. 41 (2002) 5659-5666.

[45] K. Zhang, D.S. Auld, Structure of binary and ternary complexes of zinc and cobalt carboxypeptidase A as determined by X-ray absorption fine structure. Biochemistry 34 (1995) 16306-16312.

[46] M.D. Joshi, G. Sidhu, I. Pot, G.D. Brayer, S.G. Withers, L.P. Mclntosh, Hydrogen bonding and catalysis: a novel explanation for how a single amino acid substitution can change the pH optimum of a glycosidase. J. Mol. Biol. 299 (2000) 255-279.

Figure Legends

Fig. 1. Structure of MMP-7. The MMP-7-hydroxamate inhibitor complex (Protein Data Bank no. 1MMQ) [4] was drawn using Swiss-Pdb Viewer 4.0. The active-site zinc ion is shown as a sphere. (A) Overall structure. Peptide chain is represented by a ribbon. The side chains of Glu198, Tyr193, Tyr216, and Tyr219 and the hydroxamate inhibitor are shown as a stick. (B) Close-up view of the active site. The side chains of Glu198 and Tyr219, the main and side chains of Ala162 and Pro217, and the two water molecules (W1 and W2) are shown as a ball and stick. The hydroxamate inhibitor is shown as a wire with the nearest two oxygen atoms to the active-site zinc ion as a ball. The number indicates that of the amino acid residues.

Fig. 2. Reaction scheme for the pH-dependence of MMP-7 activity with two ionizable groups involved in enzyme activity. E, S, H, and P denote MMP-7, the substrate, proton, and the product, respectively. K_{e1} and K_{e2} are proton dissociation constants of the ionizable groups of the free MMP-7, respectively, and K_{es1} and K_{es2} are proton dissociation constants of the MMP-7 combined with substrate, respectively [27,34].

Fig. 3. Titration curve of pH of L-Glu solution. The titration was carried out at 25 (open circle), 35 (open square), and 45°C (open triangle). The degree of dissociation of L-Glu at each pH was calculated by Eq. 7. The pK_{a1} and pK_{a2} were calculated by Eq. 10, which were 2.1 ± 0.1 and 4.0 ± 0.1 for 25°C, 2.2 ± 0.1 and 4.1 ± 0.1 for 35°C, and 2.3 ± 0.1 and 4.2 ± 0.1 for 45°C, respectively. Inset shows van't Hoff plot for pK_{a2} of L-Glu. Enthalpy change, ΔH^{o}, of deprotonation was calculated to be -23.6 ± 5.8 kJ mol^{-1}. One of the representative data is shown.

Fig. 4. Effect of pH on the wild-type MMP-7-catalyzed hydrolysis of MOCAc-PLGL(Dpa)AR. The reaction was carried out at 15 (open circle), 25 (open square), 35 (open triangle), and 45°C (open diamond), each with the initial enzyme and substrate concentrations of 10 nM and 1.5 μM, respectively. The relative k_{cat}/K_m is defined as the ratio of the k_{cat}/K_m at the indicated pH to that at the optimal pH (1.63×10^{-4} M^{-1} s^{-1} at pH 6.8 for 15°C, 4.01×10^{-4} M^{-1} s^{-1} at pH 6.8 for 25°C, 5.39×10^{-4} M^{-1} s^{-1} at pH 6.6 for 35°C, and 7.77×10^{-4} M^{-1} s^{-1} at pH 6.0 for 45°C). Error bars indicate SD values. One of the representative data is shown.

Fig. 5. van't Hoff plot for pK_e of MMP-7. pK_{e1} (A) and pK_{e2} (B) values of MMP-7 were plotted against the reciprocal of the absolute temperature. Error bars indicate SD values. Enthalpy change, ΔH^o, of deprotonation was calculated from the slope: (A) -20.6 ± 6.1 kJ mol^{-1}; (B) 89.9 ± 4.0 kJ mol^{-1}. One of the representative data is shown.

Fig. 6. Effect of pH on the MMP-7 variants-catalyzed hydrolysis of MOCAc-PLGL(Dpa)AR at 25°C. The reaction was carried out with the wild-type MMP-7 (open circle), A162G (open square), and P217G (open triangle). The initial enzyme and substrate concentrations were 10 nM and 1.5 μM, respectively. The relative k_{cat}/K_m is defined as the ratio of the k_{cat}/K_m at the indicated pH to that at the optimal pH (4.01×10^{-4} M^{-1} s^{-1} at pH 6.8 for the wild-type MMP-7, 2.46×10^{-4} M^{-1} s^{-1} at pH 6.8 for A162G, and 3.18×10^{-4} M^{-1} s^{-1} at pH 7.0 for P217G). Error bars indicate SD values. One of the representative data is shown.

595 Fig. 7. Proposed mechanism for the MMP-7-catalyzed cleavage of peptides. See the text
596 for details.
597

A

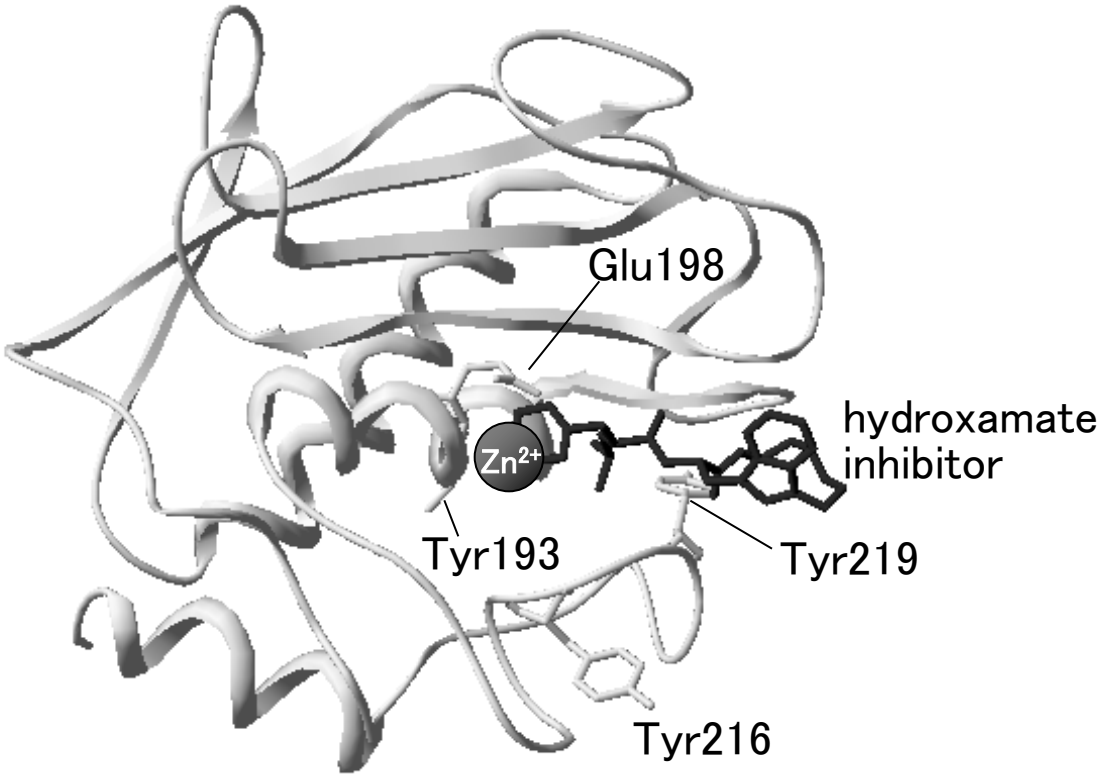

Fig. 1

B

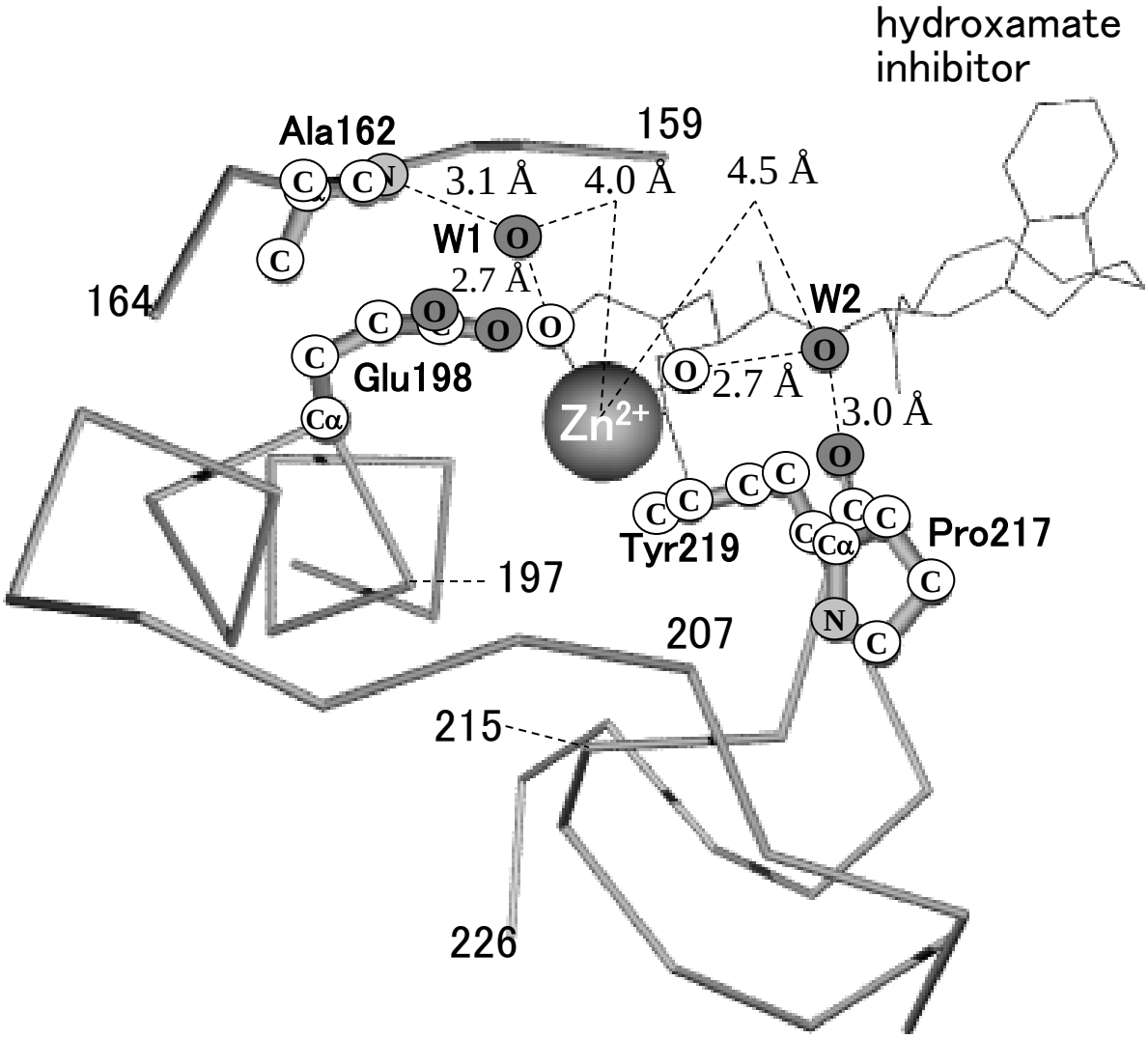

Fig. 1

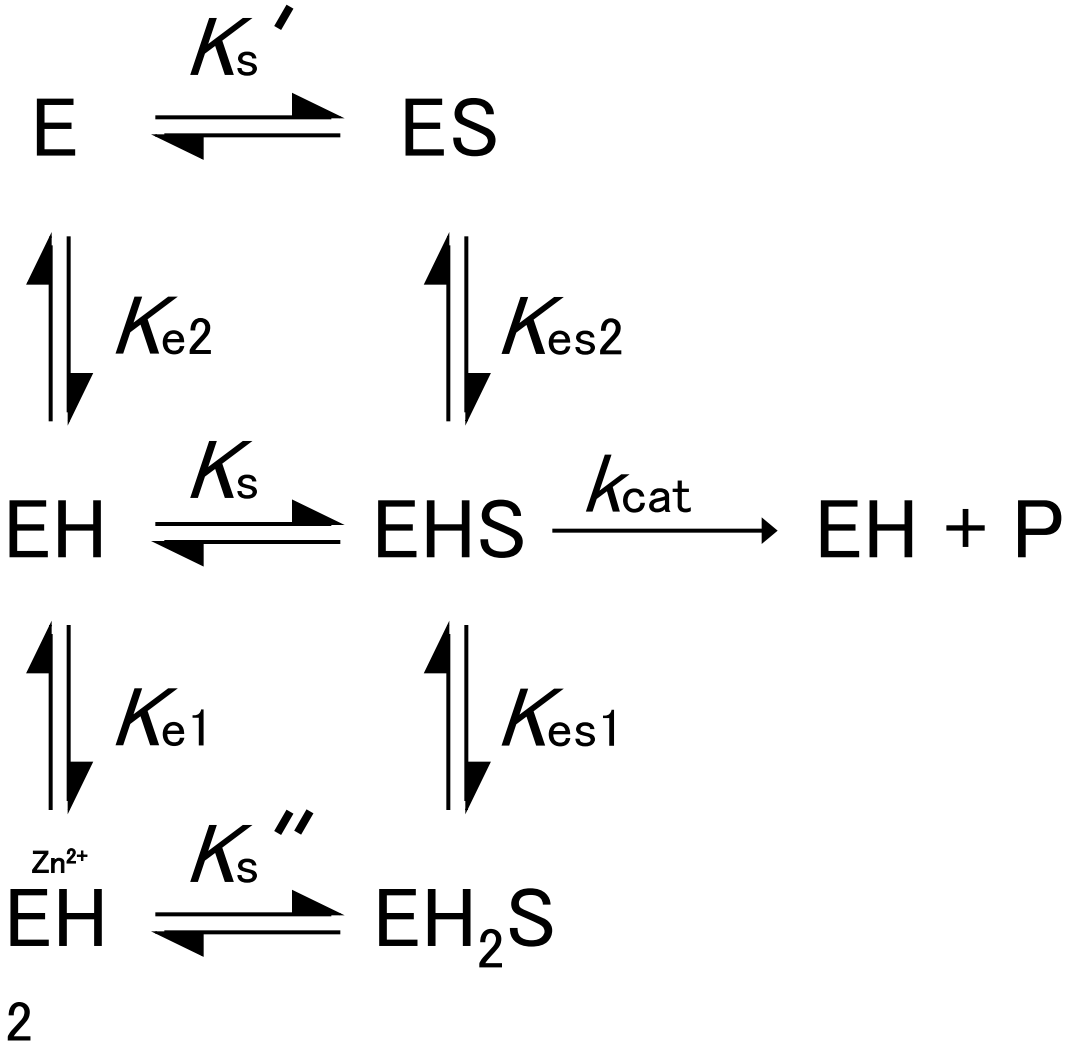

Fig. 2

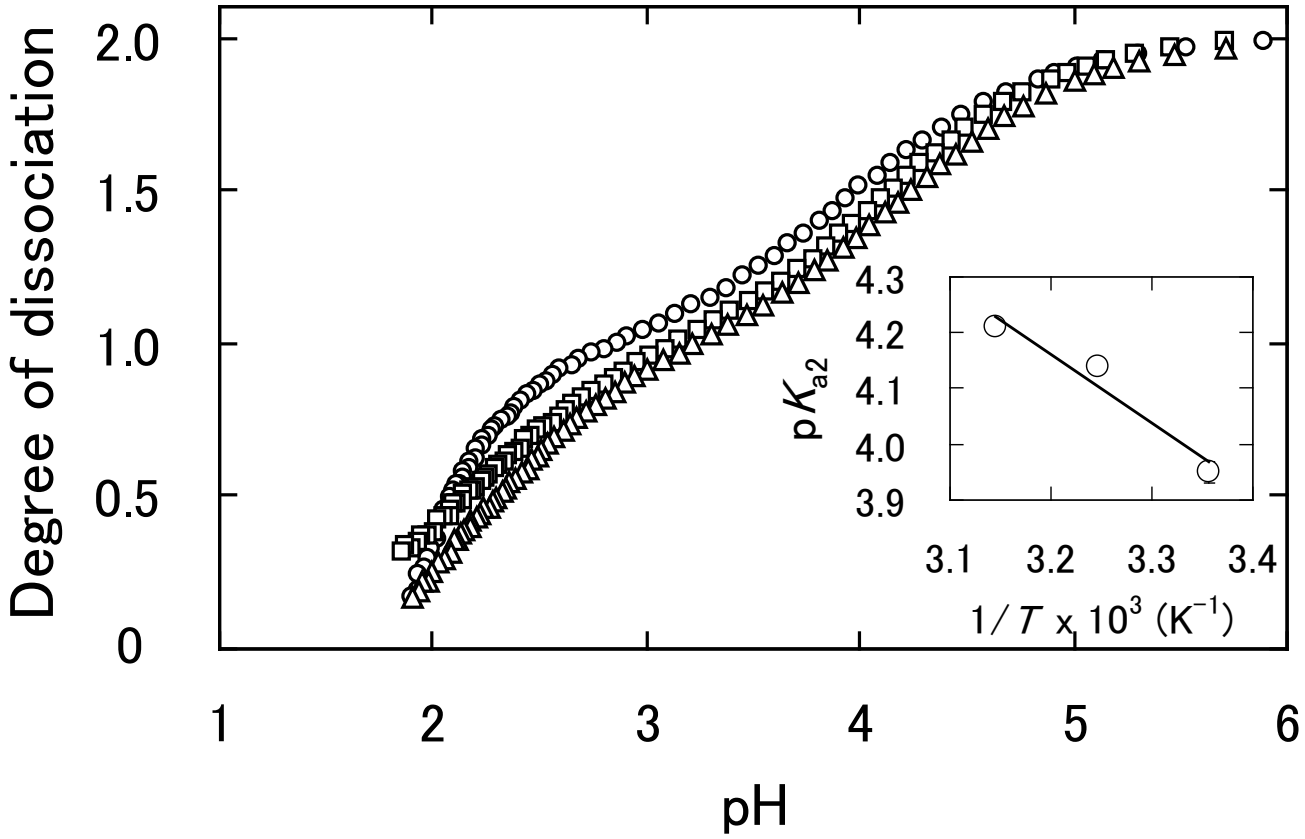

Fig. 3

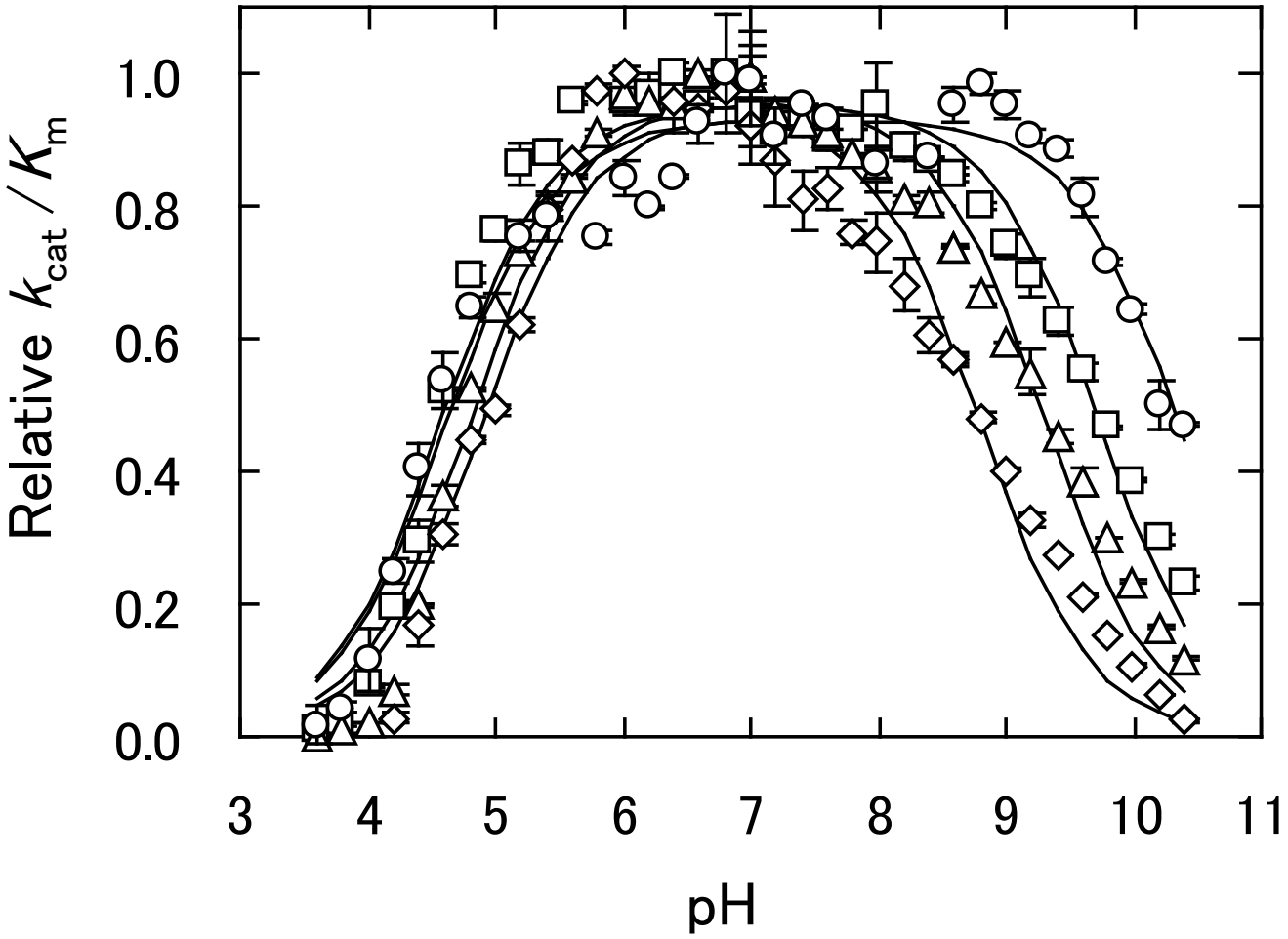

Fig. 4

A

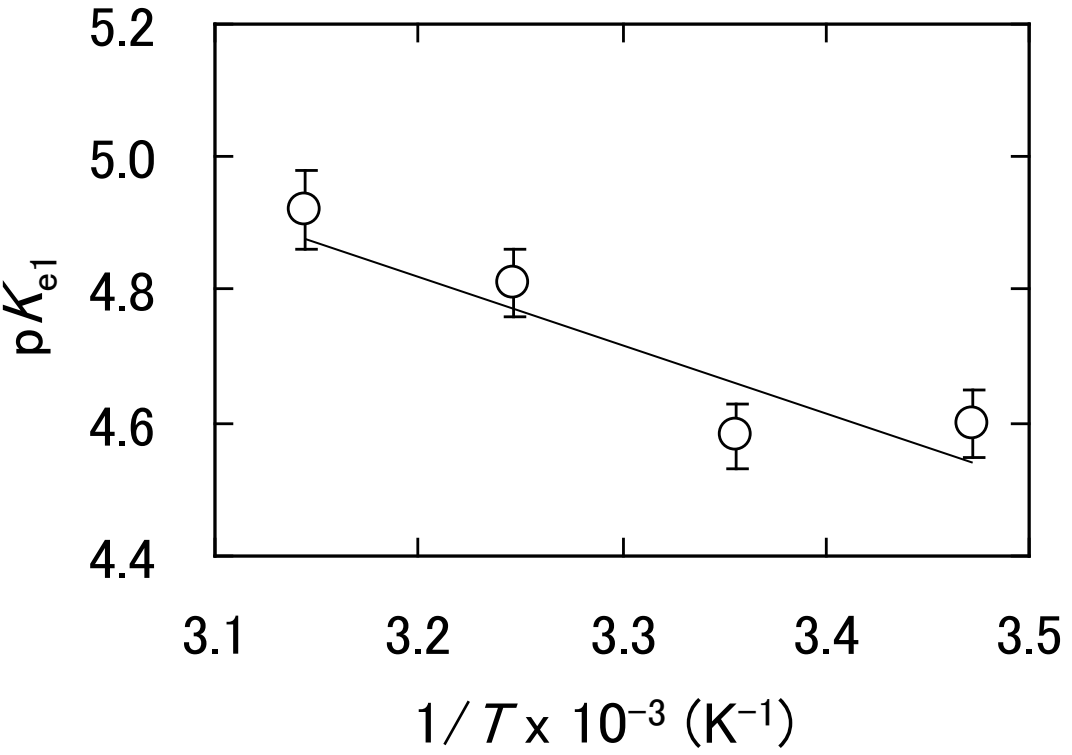

B

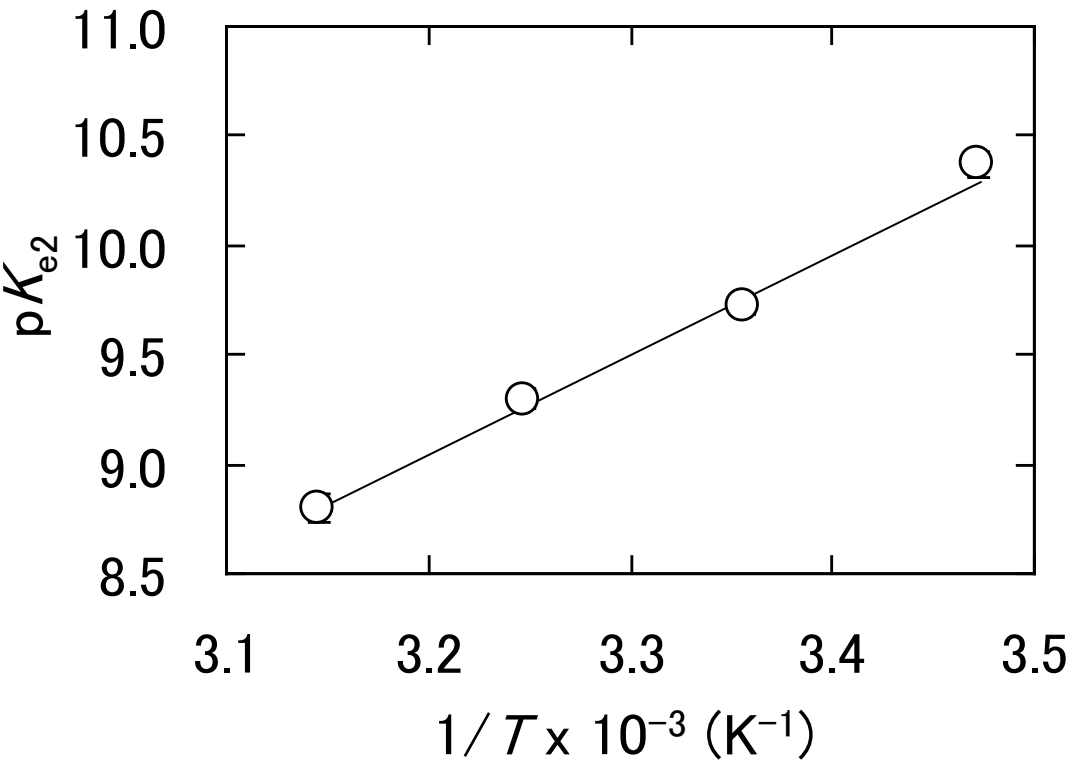

Fig. 5

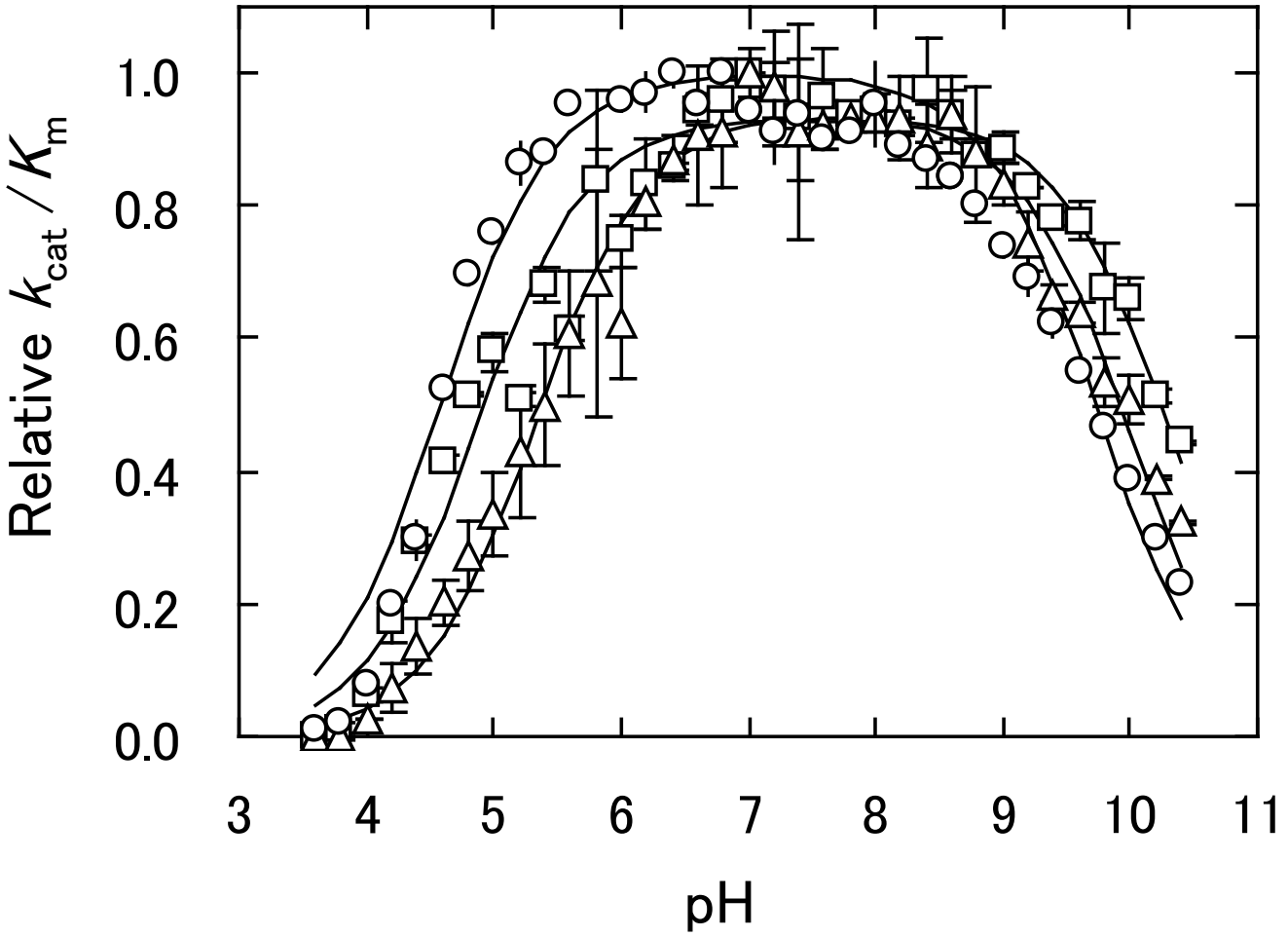

Fig. 6

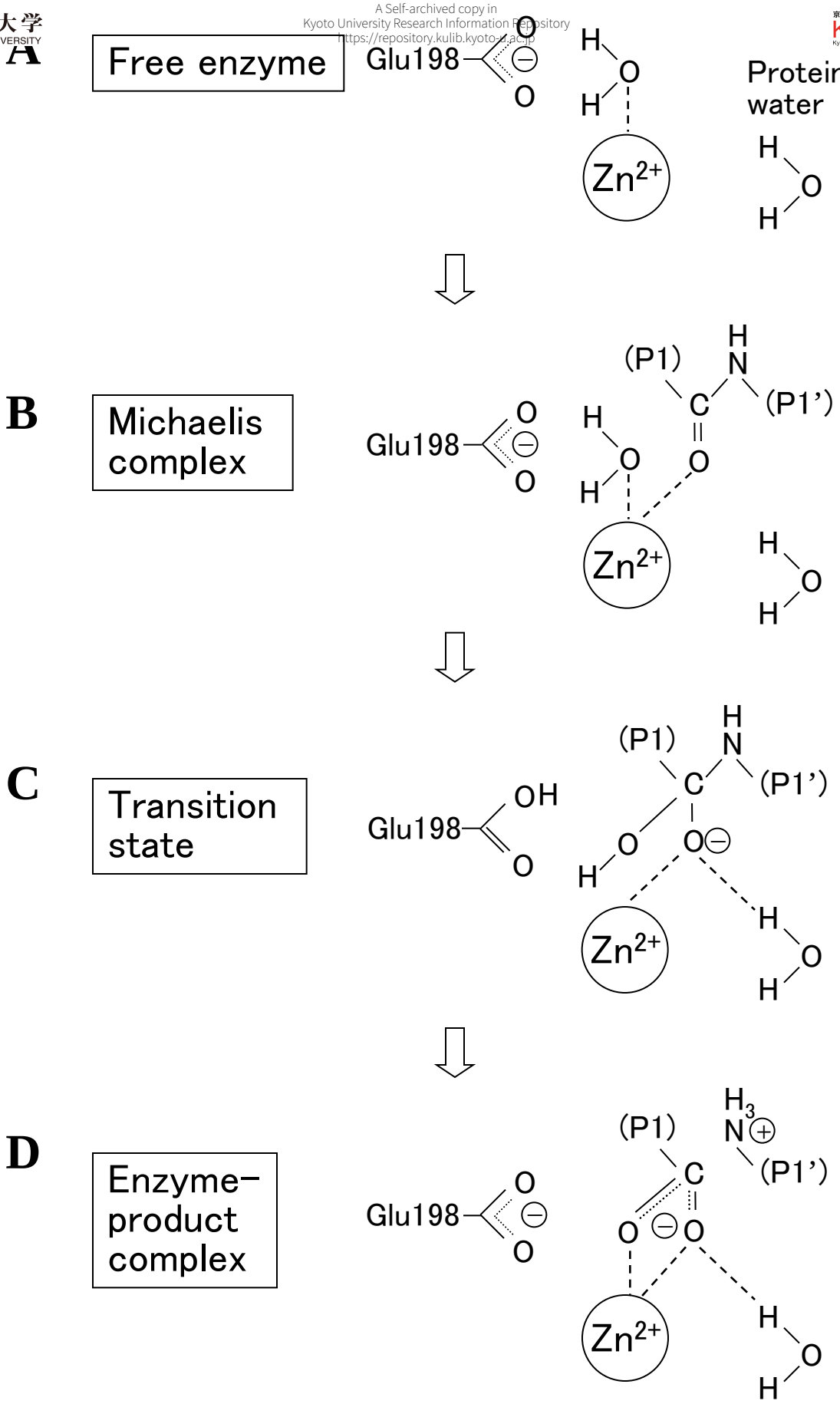

Fig. 7